New Lower Limits on the Lifetime of Heavy Neutrino Radiative Decay

S. Cecchini[a,b,c], D. Centomo[a], G. Giacomelli[a,b], R. Giacomelli[b], M. Giorgini[a,b], L. Patrizii[b], V. Popa[d,1], C.G. Şerbănuţ[e,f]

[a] *Dipartimento di Fisica dell'Università di Bologna, I-40127, Bologna, Italy*
[b] *INFN Sezione di Bologna, I-40127, Bologna, Italy*
[c] *IASF/INAF, I-40129 Bologna, Italy*
[d] *Institutul de Ştiinţe Spaţiale, R-77125, Bucharest-Măgurele, Romania*
[e] *Dipartimento di Fisica Generale dell'Università di Torino, I-10125, Torino, Italy*
[f] *INFN Sezione di Torino, I-10125, Torino, Italy*

Abstract

The data collected during the 2006 total solar eclipse are analyzed in the search for signals produced by a hypothetical radiative decay of massive neutrinos. In the absence of the expected light pattern, we set lower limits for the massive neutrino components proper lifetime. The reached sensitivity indicates that these are the best limits obtainable with this method.

Key words:
Solar neutrinos, Radiative decays of massive neutrinos, Neutrino mass and mixing, Total solar eclipses, Image processing
PACS: 96.60.Vg, 13.35. Hb, 14.60 Pq., 95.85.Ry, 95.75.Mn

1. Introduction

The evidence for solar and atmospheric neutrino oscillations [1-5] implies that neutrinos have non-vanishing masses, and that neutrino flavour eigenstates are superpositions of mass eigenstates. D.W. Sciama pointed out the possibility of ν radiative decay and the observational and theoretical consequences [6]. Massive neutrinos could undergo radiative decays; a possible decay mode is $\nu_2 \rightarrow \nu_1 + \gamma$.

Email address: vpopa@spacescience.ro (V. Popa)
[1] Corresponding author

The neutrino radiative decay requires a non-vanishing neutrino magnetic moment; stringent existing limits ($\mu_\nu < 0.9 \cdot 10^{-10} \mu_B$, [7]) apply to neutrino flavour eigenstates and cannot be directly extended to dipole magnetic moments of neutrino mass eigenstates.

"Semi-indirect" limits on neutrino radiative decay have been obtained from solar and atmospheric neutrino data. The current interpretation of existing observations is that of neutrino flavour oscillations, but the contribution from neutrino decays as a secondary effect cannot be excluded. From the SNO solar neutrino data, in ref. [8] a lower limit of $\tau_0/m > 8.7 \cdot 10^{-5}$ s/eV was inferred (τ_0 and m are the proper lifetime and mass of a decaying neutrino, respectively). By combining available solar neutrino data, limits of $\tau_0/m > 2.8 \cdot 10^{-5}$ s/eV [9], or, following different assumptions, $\tau_0/m > 10^{-4}$ s/eV [10] were obtained.

Direct searches for radiative (anti)-neutrino decays were performed in the vicinity of nuclear reactors (e.g. [11], yielding limits between $\tau_0/m > 10^{-8}$ s/eV and $\tau_0/m > 0.1$ s/eV, for $\Delta m/m$ between 10^{-7} and 0.1); the Borexino Counting Test Facility at Gran Sasso yielded limits at the level of $\tau_0/m \sim 10^3$ s/eV [12].

Cowsik [13] pointed out that astronomical observations at x-ray, optical and radio-frequencies could be used to derive bounds on radiative lifetimes on the basis of the non-observation of the final γ-ray. More recently bounds have been deduced from infra-red background measurements. Such lower limits are large (e.g. $\tau_0/m > 2.8 \cdot 10^{15}$ s/eV [14]), but they are indirect and rather speculative.

The Sun is a strong source of ν_e neutrinos; the expected flux at the Earth (neglecting oscillation effects) is $\Phi \simeq 7 \cdot 10^{10}$ cm^{-2}s^{-1}. If radiative neutrino decays occur yielding visible photons, they would not be observable due to the very large amount of solar light. During a Total Solar Eclipse (TSE) the Moon screens the direct light from the Sun, while it is completely transparent to solar neutrinos. An experiment looking for such an effect would thus be sensitive to neutrino decays occurring between the Moon and the Earth.

In a pioneering experiment performed in occasion of the October 24, 1995 TSE, a first search was made for visible photons emitted through radiative decays of solar neutrinos during their flight between the Moon and the Earth [15]. The authors assumed that all neutrinos have masses of the order of few eV, $\Delta m^2_{12} \simeq 10^{-5}$ eV^2, an energy of 860 keV and that all decays yield visible photons, which travel nearly in the same direction as the parent neutrinos. From the absence of a positive signal they estimated a lower limit on τ_0 (97

s) which, in view of the assumptions made, is now not reliable.

We made a search for solar neutrino radiative decays during the June 21, 2002 TSE, in Zambia [16] after a first attempt during the 1999 eclipse in Romania [17]. The proper lower time limits (95% C.L.) obtained for the $\nu_2 \to \nu_1 + \gamma$ decays of left-handed neutrinos ranged from $\tau_0/m_2 \simeq 10$ to $\simeq 10^9$ s/eV, for 10^{-3} eV $< m_1 <$ 0.1 eV.

In this paper we report on the observations performed in occasion of the 29 March 2006 TSE, from Waw an Namos, Libya.

2. The experimental setup

2.1. The main observation system

Our main system used a Matsukov-Cassegrain telescope (Φ = 235 mm, f = 2350 mm) equipped with a fast 16 bit Mx916 CCD camera. The original findscope was substituted by the digital videocamera used for data taking during the 2002 TSE.

The night before the eclipse we aligned the system, adjusted the focus and took calibration images of some standard luminosity stars (SAO99215 and SAO99802). In order to avoid the over-heating of the telescope and CCD and to minimize the possibility of focus and alignment changes, the equipment was protected with aluminum foils. A photograph of the set up is shown in Fig. 1. Pictures of our set ups as well as data evaluation may be found in ref. [18].

The telescope movement was set to follow the Sun in order to have always the center of the acquired images coincident with the Sun center. Furthermore, we implemented a special CCD exposure algorithm in order to adapt the exposure times to the luminosity level of the Moon image. The ashen light (the Sun's light reflected by the Earth back to the Moon) is one of the main background sources in such searches, but it allows the reconstruction, frame by frame, of the real position of the Sun behind the Moon, eliminating the risk of pointing errors due to undesired movements of the telescope.

2.2. The backup systems

The digital video-camera used in occasion of the 2002 TSE was a small backup system. It produced a digital film of the eclipse that could confirm our earlier results [16].

Figure 1: A photo of the main system deployed in the Libyan Sahara desert. The telescope, the CCD and the digital videocamera are visible. The aluminum foil reduced the heating of the apparatus. The solar filter on the top of the telescope was used only during the partiality.

A smaller Celestron C5 telescope equipped with a manually controlled digital camera (Canon D20) was also used. We obtained 50 digital pictures of the eclipse.

In this paper we discuss only the data collected with the main system, which has a much higher sensitivity than the back-up systems.

3. The experimental data

On the 29^{th} of March 2006 we observed the total solar eclipse from a location (17.960° East longitude, 24.496° North latitude and 465 m altitude) in the Libyan Sahara desert, practically on the totality line and very close to the maximum eclipse point. The time of the totality was close to noon, so the Sun and the Moon were near their highest positions in the sky (about 65.5°), corresponding to the minimum light absorption by the atmosphere.

The data collected by the main system consist in 212 digital pictures of the central part of the "dark" disk of the Moon. We used a 2×2 binning in order to maximize the CCD sensitivity keeping at the same time a good spatial resolution. Each image pixel covers (in arc second squared) a solid

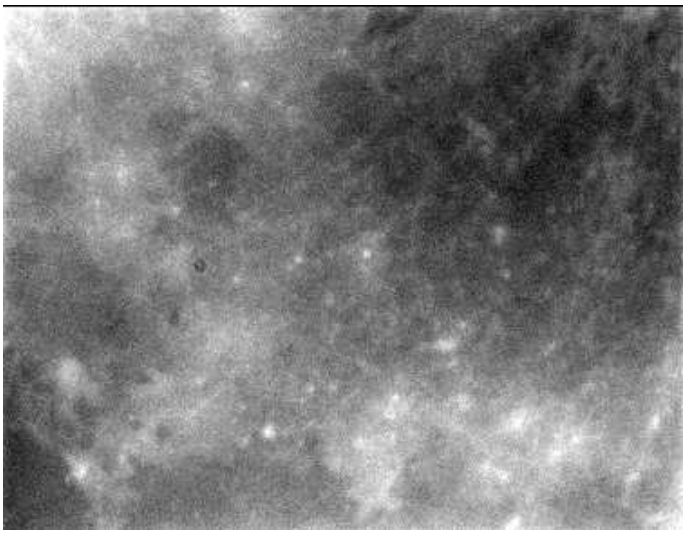

Figure 2: One of the frames recorded during the 2006 TSE. The center of the image corresponds to the position of the center of the Sun behind the Moon.

angle of 1.99" × 1.95". The analysis described in Sect. 5 is based on the wavelet decomposition of the images; we selected only the central largest dyadic square from each frame (256×256 square pixels); the total coverage was $8.49' \times 8.32'$ (the Moon apparent diameter is $31'$).

Fig. 2 shows one of the frames recorded during the totality phase; details on the Moon surface seen in the ashen light are visible.

In Fig. 3 the image of the Moon observed in the light of the Sun is compared with one of our frames (in ashen light). The corresponding area on the Moon is marked by a rectangle. Differences are due to the different Moon lighting conditions; some small scale details can be located in both images.

Dark CCD frames, used to eliminate the effect of some possible "hot pixels", were recorded before and after the totality phase.

3.1. Alignment and pointing

The telescope was aligned the night before the eclipse using the North Star (in the same observation session in which the calibration pictures were taken), and it was kept in position till the end of the eclipse.

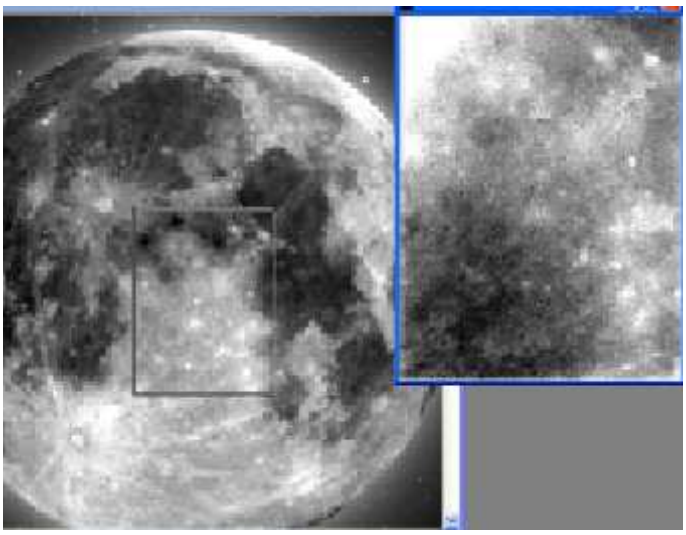

Figure 3: A full Moon picture (left) compared to one frame (right). The differences are due to the different lighting conditions: in the light of the Sun and in the ashen light, respectively. The rectangle on the Moon shows the area covered by the frame measured during the eclipse.

We continuously checked the Sun position, starting at the moment of the first contact, using a grid applied on the screen of the digital videocamera.

We used 7 luminous spots on the frames (small Moon craters reflecting the ashen light) as "fiducial" points to reconstruct for each frame the relative position of the center of the Sun. Although the telescope movement was set to follow the Sun, the human activity around our apparatus caused some ground oscillations that were corrected using the fiducial points. For the analysis we retained 195 frames in which all 7 points were clearly determined. Fig. 4a shows the displacement of the fiducial points due to the relative movement of the Moon with respect to the Sun. The arrow indicates the North direction (for the Moon). In Fig. 4b the variation of the "x" coordinate with time is shown. The origin of the time axis is at 12 hours and 13 minutes local time, about 50 seconds before the second contact of the eclipse. Small oscillations caused by human activity in the vicinity of the instrument are visible; their effect was removed in the off-line analysis.

The superposition of the selected 195 frames is shown in Fig. 5. All lunar landscape details are washed away; the light gradient is due mostly to the

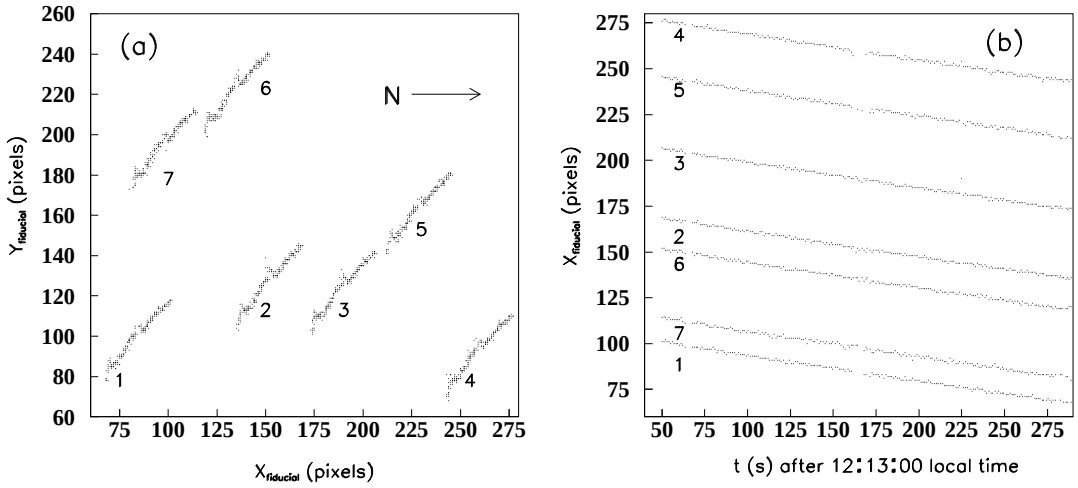

Figure 4: (a) Map of the successive positions in the CCD of 7 fiducial points on the Moon surface during the totality phase of the eclipse. The arrow indicates the Moon North direction. (b) "x" coordinates of the fiducial points versus time during the eclipse.

asymmetry of the coronal light diffracted by the Moon border and reaching the instrument. The small darker spot visible in the picture (at the center of the image, ∼1.5 cm to the left) is due to a sand grain on the telescope window. The procedure applied to eliminate all spurious effects on the image is discussed in Sect. 5.

3.2. Exposure time

The exposure time for each frame was computed to have the maximum contrast avoiding at the same time saturated pixels. The algorithm analyzed the previous frame, and computed the exposure time for the next one so that the average luminosity was in the middle of the dynamical range of the 16 bit CCD. The exposure time and other information concerning the telescope movement were registered in the headers of each frame.

For most frames the exposure time was $0.5 \div 0.6$ seconds, as expected. 40 frames had a longer exposure, ∼1 s; each of them was acquired immediately after a frame having a normal exposure time, but with a luminosity about one half of the expected one. This was probably caused by a delay in the electromechanical CCD shutter operation due to some grains of dust that made their way into the apparatus. The exposure times were corrected in the analysis requiring that the acquisition rate be the average between the

Figure 5: The superposition of the 195 selected frames used in the analysis. The center of the image corresponds to the position of the center of the Sun.

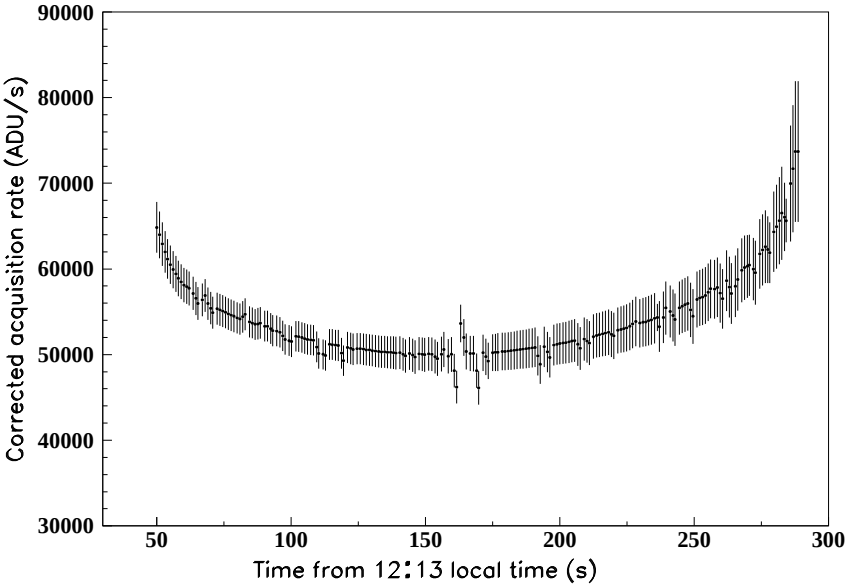

Figure 6: The exposure rate for each frame after the correction discussed in the text.

acquisition rates of two adjacent frames.

Fig. 6 shows the time dependence of the frames exposure rate in Acquisition Digital Units (ADU) per second. Larger rates at the beginning and at the end of the totality phase are due to a larger amount of coronal light diffracted by the Moon and reaching the telescope. The oscillations close to the eclipse maximum correspond to frames for which not all the 7 fiducial points could be clearly identified (this was due to people moving around the experiment). These frames were excluded from the final analysis. After the time correction and the removal of "shaken" frames, the total exposure time during the totality phase of the eclipse is about 116 seconds. The difference between this value and the duration of the totality is mainly due to the time requested to read the CCD information and transfer it to the computer.

3.3. Calibration

As mentioned in Sect. 2.1, the calibration of the main system was done the night before the eclipse using two standard luminosity stars, SAO99215 and SAO99802. We took 20 frames, 2 s exposure each, for the first star and 30 frames with the same exposure for the second star (which is slightly fainter). After the removal of the dark frames the astro-photometric measurements indicate that one ADU corresponds to 6.1 ± 0.1 photons.

4. Monte Carlo simulations

The analysis of the data obtained by this experiment required a detailed Monte Carlo simulation, including the neutrino production in the solar core, its propagation, decay, and the detection by our telescope on Earth. Such a code was developed for the analysis of the previous data collected during the 2001 eclipse [16] and was adapted to the conditions of the 2006 observations. The model is described in detail in ref. [19]; here the main ideas are summarized and the parts relevant for the 2006 eclipse.

Solar neutrino production was simulated according to the "BP2000" Standard Solar Model (SSM) [20] available in numerical form in ref. [21]. We chose a specific reaction/decay yielding neutrinos (both from the p-p and the CNO cycles); the neutrino energy and the position of its production point in the core of the Sun were generated according to the SSM. As we are interested only in neutrinos that could undergo radiative decays between the area of the Moon seen by our experiment and the Earth, a decay point was generated and the arrival direction of the decay photon was chosen. Once the

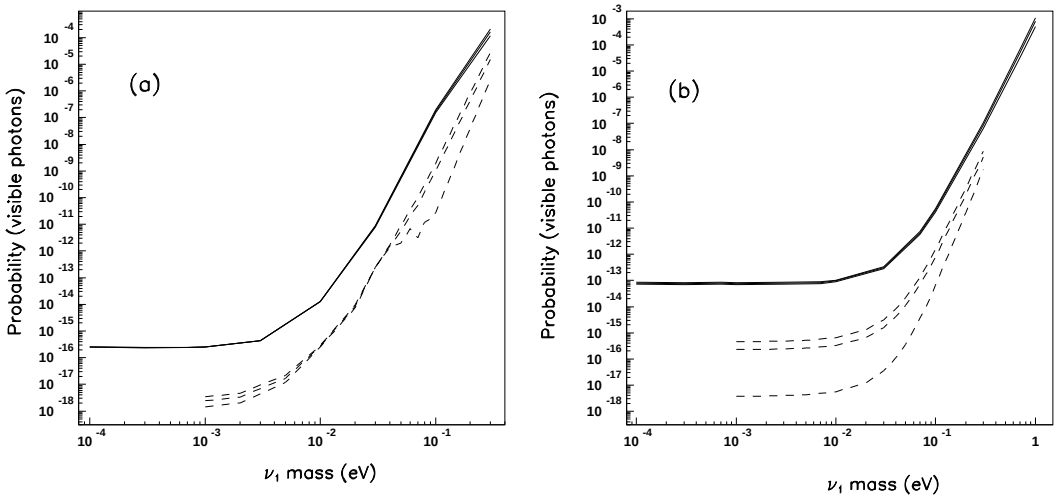

Figure 7: (a) The Monte Carlo probability to have a visible photon arriving to the telescope from the $\nu_2 \to \nu_1 + \gamma$ radiative decay, versus the ν_1 mass, in the conditions of the 2006 experiment (solid lines), compared to similar probabilities in the 2002 experiment (dashed lines). The dashed lines correspond from up to down to left-handed, Majorana and right-handed neutrinos. The differences in the probabilities for the 2006 simulation for different ν_2 polarities are too small to be seen in the graph. (b) The same as in (a) for the $\nu_3 \to \nu_{2,1} + \gamma$ decays.

geometry of the event is known, the photon energy is computed taking into account the Lorentz boost, and for visible photons the probability density of the angular distribution, depending on whether the neutrino is a Dirac neutrino, left or right-handed, or a Majorana neutrino. The number of visible photons is about $5 \cdot 10^{-4}$ of the total spectrum; this quantity is integrated over all directions accessed by the instrument aperture.

The interpretation of solar neutrino oscillation data in the simplest two flavour model (assuming that the electron neutrino ν_e is a superposition of two mass eigenstates ν_1 and ν_2) yields a square mass difference $\Delta m^2_{1,2} = 6 \cdot 10^{-5}$ eV^2 [1]. This value was used in simulating $\nu_2 \to \nu_1 + \gamma$ decays. The probabilities that the photon emitted in the space between the Moon and the Earth is a visible photon and reaches the telescope are shown in Fig. 7a, versus the ν_1 mass (solid line). For comparison, we also show the corresponding probabilities obtained in 2002 with a different system. In the conditions of the 2006 experiment, differences among neutrino polarities are smaller and cannot be observed in the scale of Fig. 7.

Assuming a mixing among all 3 mass eigenstates with $\Delta m^2_{1,3} \simeq \Delta m^2_{2,3} = 2.4 \cdot 10^{-3}$ eV^2 (as known from atmospheric neutrino [2, 3, 4] and long baseline oscillation experiments [5]), $\nu_3 \to \nu_2 + \gamma$ and $\nu_3 \to \nu_1 + \gamma$ decays should behave in the same way. The resulting probabilities are shown in Fig. 7b.

The notation of the lines is as in Fig. 7a.

The $\nu_2 \to \nu_1 + \gamma$ decays should produce a spot of light coincident with the center of the Sun behind the Moon disk, about 60" large, while the signal from the $\nu_3 \to \nu_{1,2} + \gamma$ decays would consists of light rings about 20" thick, with diameters of about 200" and 250", also centered in the Sun.

5. Data analysis

The search for $\nu_2 \to \nu_1 + \gamma$ and $\nu_3 \to \nu_{1,2} + \gamma$ signatures in the frames recorded during the 2006 total solar eclipse is based on the wavelet decomposition of the compound image, shown in Fig. 5. We recall that this image is a superposition of 195 selected 16 bit frames recorded during the TSE and aligned with respect to the center of the Sun position behind the Moon. As in the case of the 2002 eclipse [16] we chose the Haar wavelet basis [22]. The n-order term of the decomposition is obtained by dividing the $N \times N$ pixels^2 image in squares of $N/2^n \times N/2^n$ pixels^2 and averaging the luminosity in each square; the averages are then subtracted and the resulting image, the n-order residual, can be used to obtain the $(n+1)$-order term. Each decomposition term is an image that enhances the features on the corresponding scale, while the residuals yield information for smaller dimension scales.

The decay signal is searched for by averaging the luminosity of the images over concentric "rings" centered in the Sun. As the wavelet analysis requires a dyadic dimension (the number of pixels has to be an integer power of 2), we considered four pixels adjacent to the image center as "central" and then averaged the obtained luminosity profiles.

The image in Fig. 5 is 256×256 pixels^2; we used up to the 7^{th} order in the wavelet decomposition. Fig. 8 shows the luminosity distribution for the 7^{th} order residual, that may yield information on the smaller scale effects in the original image. The profile is consistent with statistical noise; the larger amplitudes near the center of the Sun and near the edges of the image are due to a smaller number of pixels available for the averaging.

None of the image decomposition terms or residuals shows structures as would be expected from solar neutrino radiative decays; thus a possible signal cannot be larger than the statistical fluctuations.

6. Results and discussions

The expected scale of the decay signal (few tens of arcseconds) suggests that the wavelet term most sensitive to $\nu_2 \to \nu_1 + \gamma$ and $\nu_3 \to \nu_{1,2} + \gamma$ decays

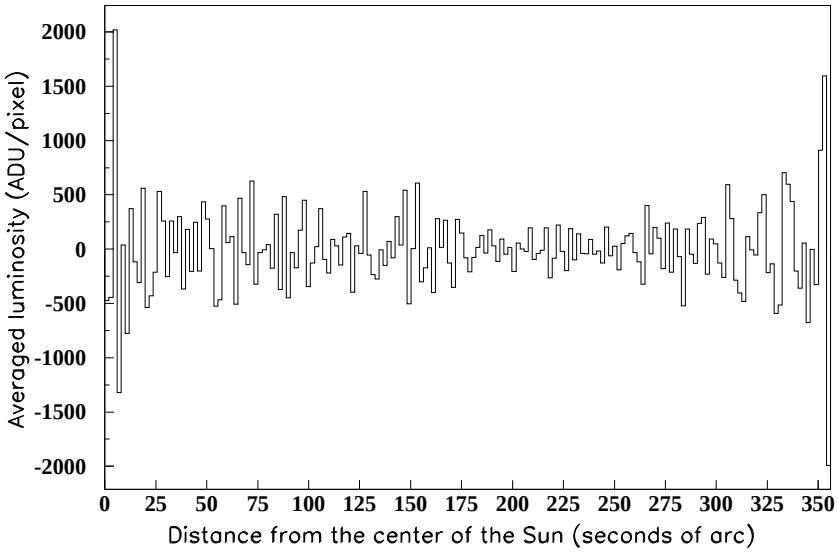

Figure 8: Luminosity profile of the 7^{th} residual from the wavelet decomposition of the central part of the Moon image in Fig. 5.

should be the 5^{th} order, with a typical scale of about 16". The number of visible photons originating from solar neutrino radiative decays that could be recorded by the telescope CCD may be computed as

$$N_\gamma = P\Phi_{(2,3)} S_M t_{obs} \left(1 - e^{\frac{\langle t_{ME}\rangle}{\tau}}\right) e^{-\frac{t_{SM}}{\tau_{(2,3)}}}, \tag{1}$$

where P is the mass-dependent probability shown in Figs. 7a,b and $\Phi_{(2,3)}$ represents the flux of ν_2 or ν_3 solar neutrinos at the Earth.

$$\begin{aligned} \Phi_2 &= \Phi_\nu \sin^2\theta_{12} \\ \Phi_3 &= \Phi_\nu \sin^2\theta_{13}, \end{aligned} \tag{2}$$

where $\Phi_\nu \simeq 7 \cdot 10^{10}$ cm^{-2}s^{-1} is the expected solar neutrino flux at the Earth (neglecting oscillations) and θ_{12} is the mixing angle in the two flavour approximation. For 3 neutrino flavours the mixing angle θ_{13} in uncertain; in our calculations we used $\sin^2\theta_{13} = 0.1$. If one used 0.06 as the 95% C.L. quoted by SNO [1], there would be only a slight reduction of sensitivity, while the reduction would be considerable in the case of $\sin^2\theta_{13} = 0.02$ [1, 7]. In Eq. 1 S_M is the area on the Moon surface covered by our observations, t_{obs} is the total acquisition time, $\langle t_{ME}\rangle$ is the average travel time of the neutrinos in the observational cone from the Moon to the Earth (assuming that the decay point is uniformly distributed along that distance $\langle t_{ME}\rangle$ is about one third

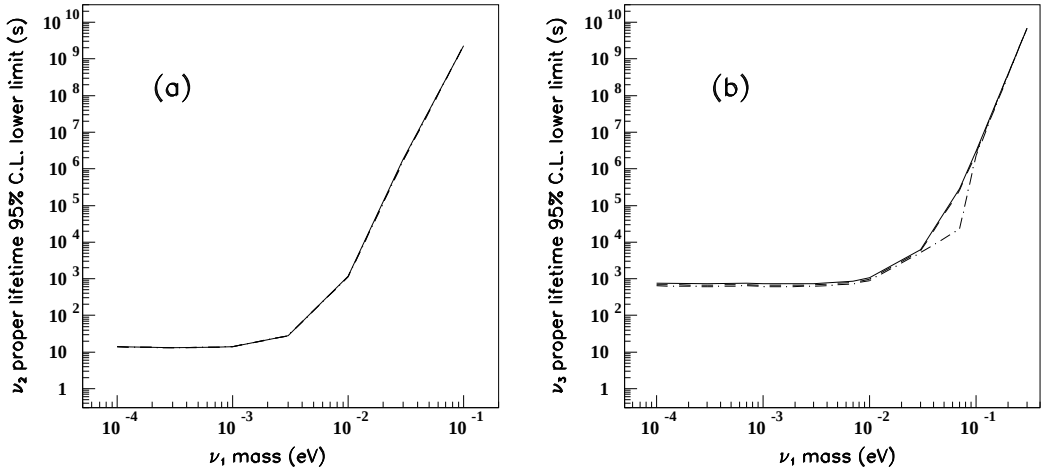

Figure 9: (a) 95% C.L. lower limits for the ν_2 proper lifetime. The differences between different polarization states cannot be seen at this scale. (b) 95% C.L. lower limits for the ν_3 proper lifetime, assuming $\sin^2\theta_{13} = 0.1$. The lines correspond from up to down to left-handed, Majorana and right-handed neutrinos.

of the flying time [16]), t_{SM} is the flight time from the Sun to the Moon and $\tau_{(2,3)}$ the lifetime of ν_2 and ν_3 neutrino mass higher states. All time variables in Eq. 1 are defined in the laboratory frame of reference.

No structure compatible with ν_2 or ν_3 radiative decays was found in our analysis; lower limits for the lifetimes of the heavy neutrino components were obtained. The number of photons produced through radiative decays between the Moon and the Earth reaching our detector is $N_\gamma \leq 3\sigma_{T5}$ (95% C.L.), where σ_{T5} is the standard deviation of the luminosity of the 5^{th} term in the wavelet decomposition of the data. The 95% C.L. lower limits for the ν_2 proper lifetimes are shown in Fig. 9a. Although they were computed assuming three possible ν_2 polarizations, the results are so close that cannot be separated on the graph. For the ν_3 proper lifetimes, the 95% C.L. upper limits, computed assuming $\sin^2\theta_{13} = 0.1$, are shown in Fig. 9b. The solid line corresponds to left-handed Dirac neutrinos, the dash-dotted line to Majorana neutrinos and the dashed line to right-handed Dirac neutrinos.

7. Conclusions

The analysis of 195 frames recorded in occasion of the 26^{th} of March 2006 total solar eclipse in the Libyan Sahara desert did not evidence any signal

compatible with the Monte Carlo predictions for the radiative decays of the heavier components of solar neutrinos [19].

For $\nu_2 \rightarrow \nu_1 + \gamma$ radiative decay the 95% C.L. lower lifetime limits are in the range $10 \div 10^9$ s, for neutrino masses $10^{-4} < m_{\nu 1} < 0.1$ eV. These limits represent an improvement of about $2 \div 3$ orders of magnitude in the lower neutrino mass region with respect to our previous results [16]. Similar improvements were obtained for the $\nu_3 \rightarrow \nu_{2,1} + \gamma$, but the limits are tentative since the mixing angle θ_{13} is still uncertain.

The limits mentioned above are obtained from the fifth order wavelet term of the summed image of Fig. 5. The detection of the ashen light combined with the negative result prove that the searched signal should be fainter than the ashen light itself; we thus can state that the limits presented in this paper are the best obtainable using this technique, since there is no way to avoid the ashen light background.

Acknowledgments

We would like to acknowledge many colleagues for useful comments and discussions. The experiment was funded by the University and INFN Section of Bologna. We acknowledge also the support from the Italian Institute of Culture of Tripoli. The analysis was partially funded under CNCSIS Contract 539/2009. We are grateful to the organizers of the SPSE 2006 event for their efforts that allowed to perform our experiment. Special thanks are due to the Winzrik Group and to the Libyan Air Force for their assistance.

References

References

[1] Q.R. Ahmad *et al.* (SNO Coll.), Phys. Rev. Lett. **89** (2002) 011301.
B. Aharmim *et al.*, arXiv:0910.2984 [nucl-ex].

[2] W.W. Allison *et al.* (SOUDAN2 Coll.), Phys. Lett. **B449** (1999) 137;
Phys. Rev. **D72** (2005) 052005.

[3] M. Ambrosio *et al.* (MACRO Coll.), Phys. Lett. **B434** (1998) 451;
Phys. Lett. **B517** (2001) 59; Eur. Phys. J **C36** (2004) 323.

[4] Y. Fukuda *et al.* (SuperK Coll.), Phys. Rev. Lett. **81** (1998) 1562;
Y. Ashie *et al.*, Phys. Rev. **D71** (2005) 112005.

[5] P. Adamson *et al.* (MINOS Coll.), Phys. Rev. Lett. **101** (2008) 131802.

[6] A. L. Melott and D.W. Sciama, Phys. Rev. Lett. **46** (1981);
D.W. Sciama, Nucl. Phys. Proc. Suppl. **38** (1995) 320.

[7] C. Amsler *et al.* (P.D.G.), Phys. Lett. **B667** (2008) 1.
G.L. Fogli *et al.*, arXiv:0905.3549 [hep-ph].

[8] A. Bandyopadhayay *et al.*, Phys. Lett. **B555** (2003) 33.

[9] A.S. Joshipura *et al.*, Phys. Rev. **D66** (2002) 113008.

[10] J.F. Beacon and N.B. Bell, Phys. Rev. **D65** (2002)113009.

[11] B. Bouchez *et al.*, Phys. Lett. **B207** (1988) 217.

[12] A.V. Derbin and O.Ju. Smirnov, JETP Lett. **76** (2002) 483.

[13] H.L. Shipman and R. Cowsik, Ap. J. **247** (1981) L111.

[14] S.A. Bludman, Phys. Rev. **D45** (1992) 4720.

[15] C.D. Birnbaum *et al.* Phys. Lett. **B397** (1997) 143.

[16] S. Cecchini *et al.*, Astropart. Phys. **21** (2004) 183.

[17] S. Cecchini *et al.*, Astrophys. Space Sci. **273** (2000) 35.
S. Cecchini *et al.*, Astrophys. Space Sci. **282** (2002) 235, hep-ex/0011048.

[18] S. Cecchini *et al.*, hep-ex/0606037, Proc. Int. Symp. on Solar Physics and Solar Eclipses (SPSE2006), Sebha Univ. Publ., Sebha, Libya (2007), *http://www.irsol.ch/spse/spse-papers.php*.
Other details at *http://www.scienzagiovane.unibo.it/eclisse.html*.

[19] S. Cecchini *et al.*, Astropart. Phys. **21** (2004) 35.

[20] J.N. Bahcall, M.H. Pinsonneault and S. Basu, Ap. J. **555** (2001) 990.

[21] *http://www.sns.ias.edu/∼jnb/*.

[22] Y. Fujywara and J. Soda, prog. Theor. Phys. **95** (1996) 1059.